Edge measurements during ICRF heating on the PLT Tokamak

1990 Plasma Phys. Control. Fusion 32 51

(http://iopscience.iop.org/0741-3335/32/1/005)

Plasma Physics and Controlled Fusion, Vol. 32, No. 1, pp. 51 to 70, 1990
Printed in Great Britain.

0741-3335/90 $3.00+ .00

EDGE MEASUREMENTS DURING ICRF HEATING ON THE PLT TOKAMAK

I. S. LEHRMAN,* P. L. COLESTOCK, D. H. MCNEILL,† G. J. GREENE, S. BERNABEI, J. C. HOSEA, M. ONO, J. L. SHOHET‡ and J. R. WILSON
Princeton Plasma Physics Laboratory, Princeton University, Princeton, NJ 08543, U.S.A.

(*Received* 29 *March* 1989; *and in revised form* 8 *August* 1989)

Abstract—Edge measurements have been conducted on the PLT Tokamak under a variety of operating conditions in order to ascertain the relevant processes at work in coupling r.f. power to plasmas. The edge density is found to increase significantly with the application of ICRF, and electron heating occurs in the vicinity of the Faraday shield surrounding the antenna. Spectroscopic measurements indicate that the energized antenna is a significant particle source. The relative increase of metallic impurities was found to be ~2.7 times larger than the corresponding increase in deuterium. In addition, the relative increase of deuterium and impurities was ~3–4 times greater at the energized antenna than at other locations around the torus. Model calculations show that for deuterium released from the Faraday shield, the D_α emission is localized radially to a region within 4 cm of the antenna. A correlation was found between the edge density and the D_α intensity that justifies its use as a measure of the particle source rate.

1. INTRODUCTION

AUXILIARY HEATING has become a major research effort in the magnetic fusion energy program because present research devices have been unable to reach fusion temperatures via Ohmic heating. Neutral beam injection (NBI) has been successful in heating plasmas close to thermonuclear conditions, though beam penetration is not expected to scale favorably to the high densities and temperatures associated with thermonuclear conditions. An additional difficulty with NBI is the unavoidable neutral particle input, rendering plasma density control very difficult. Ion cyclotron range of frequency (ICRF) heating is one of the current technologies being investigated for heating plasmas to ignition conditions that has shown promise with its favorable experimental results and its ability to penetrate into the core of high density plasmas (COLESTOCK, 1984; ADAM, 1987; STEINMETZ *et al.*, 1979). The frequency of a reactor ICRF heating system will lie in the range 50–100 MHz where efficient, high-power radio frequency sources are readily available (RAWLS, 1982). Another technology benefit of ICRF heating is that the r.f. generators need not be located close to the reactor, unlike NBI, but may be remotely situated in a non-radioactive environment with the r.f. power delivered to the reactor via standard coaxial transmission lines. An ICRF antenna, which couples the r.f. energy to the plasma, could be of modular design, mounting onto a rectangular port in the reactor vessel wall. The modular construction would also simplify the maintenance procedure in radioactive areas.

Although promising, ICRF heating is not without its own set of complications. The desired ion heating is often accompanied by a number of undesired side effects which,

* Permanent address: Grumman Corporate Research Center, 4 Independence Way, Princeton, NJ 08540, U.S.A.
† Present address: Princeton Research Forum, P.O. Box 497, Princeton, NJ 08542, U.S.A.
‡ Permanent address: University of Wisconsin–Madison, Madison, WI 53706, U.S.A.

if not controlled, could limit the usefulness of ICRF heating in reactor-sized devices. The most notable effects are an increase in the impurity concentration and an uncontrolled rise in the plasma density (COLESTOCK *et al.*, 1985). The increase in impurity concentration results in enhanced Bremsstrahlung, recombination, and spectral line radiation losses. It also depletes the reacting hydrogenic ion species. These losses result in a significant reduction of the energy confinement time, making ignition conditions more difficult to obtain. The density rise is undesirable since it can be large enough to cause complete disruption of the discharge as the density limit of a given device is surpassed (MURAKAMI *et al.*, 1976).

It is worth mentioning that recent experiments have reported on the favorable use of wall and antenna conditioning to reduce, and in some cases suppress, the deleterious side effects of ICRF heating. TEXTOR has utilized extensive carbonization of the vessel wall which resulted in discharges characterized by stationary plasma parameters and negligible increase in impurity radiation (MESSIAN *et al.*, 1976). TEXTOR has also investigated the use of boronization to reduce the density rise and impurity production (BEUKEN *et al.*, 1988; RINGER *et al.*, 1988). The boronization process reduced the radiated power by 25% with the density remaining nearly flat for the duration of the 1.6 s, 2.6 MW r.f. pulse. The beneficial effects of the boronization were found to last for more than 200 discharges.

To identify the relevant processes at work in coupling ICRF power to plasmas, a number of experimental measurements have been made on the, now defunct, Princeton Large Torus (PLT) Tokamak. The time evolution of the bulk plasma parameters and the edge plasma parameters were measured under a variety of operating conditions. Langmuir probe measurements of edge electron temperature and density were made and compared at several locations around the torus. In addition to these measurements, spectroscopic measurements of deuterium, carbon, chromium and iron were made in order to identify significant particle sources during ICRF heating. The purpose of the edge measurements was to characterize changes in the edge plasma and to determine any correlations with the bulk plasma.

A major difficulty in obtaining these data was the condition of the antennas and the vacuum vessel, which placed an operational limit on the power levels achievable for these experiments. Though most of the results presented here are from relatively low-power experiments ($P_{\text{r.f.}} < 1$ MW), these experiments are appropriate for characterizing the edge plasma since the deleterious side effects associated with ICRF heating on PLT are observable at most all power levels (COLESTOCK *et al.*, 1985).

2. APPARATUS

The PLT Tokamak had a major radius $R = 132$ cm, and a minor radius a, which was determined by a pair of graphite limiters which were nominally set at 40 cm. The discharges used as target plasmas for the ICRF heating experiments were of the following type: the toroidal magnetic field, B_t, was typically 30 kG, the plasma current, I_p, was typically 600 kA, and the line-averaged plasma density, $\bar{n}_e$, ranged from 1 to 6×10^{13} cm^{-3}. The main plasma constituent for the PLT experiments was deuterium. The discharges lasted ~ 1 s with a flat-top stage, where the parameters of the discharge remained relatively constant, lasting ~ 600 ms. ICRF heating experiments were conducted during the flat-top stage of the discharge with an r.f. pulse lengths of 50–200 msec. The parameters of the discharge were varied, as well as the r.f. power levels, to

investigate correlations between the edge and bulk plasma. A further description of PLT and its operating regime can be found in FURTH (1979), GROVE *et al.* (1976) and THOMPSON (1984).

The ICRF antennas utilized in the PLT experiments consisted of half-turn loops mounted in the edge region, 5 cm above the vessel wall. As depicted in Fig. 1, the loops were surrounded by top and bottom Faraday shield elements. The toroidal extent (z direction) of the shield was approximately 10 cm. The poloidal separation of the top layer shield elements was 0.5 cm, while the poloidal extent was 1 cm. The separation between the top and bottom layers was 0.5 cm.

The plasma density was controlled by a gas feedback system. The application of ICRF power was most often accompanied by a particle influx which was large enough so as to increase the overall plasma density above the desired level. At times, the density rise caused the discharge to disrupt. Titanium gettering was employed between discharges in an attempt to reduce the impurity concentration and the density rise, though it was of limited benefit.

In order to characterize changes that occurred in the edge plasma during ICRF heating experiments, a number of diagnostics were employed. In addition to the standard set of diagnostics routinely used on PLT, a double Langmuir probe was used to measure the edge electron temperature and density, and visible spectroscopic measurements of deuterium and impurities were made. Discharges were repetitively produced while probe positions were varied from shot to shot to determine the spatial properties of the edge plasma. The double Langmuir probe, shown in Fig. 2a, consisted of two coaxial lines with center conductors which extended 6 mm past the outer conductor. The inner conductors were made from tungsten wire, 1.5 mm diameter. The coaxial lines were inserted into a graphite rod to avoid damage from the plasma. All connections to the probe were made with coaxial lines in order to reduce r.f. pick-up. The bias circuit for the double probe is shown in Fig. 2b. An isolation transformer driven from the 120 V, 60 Hz mains provided the bias for the probes.

The probe was held at a fixed radial location during a discharge and the applied voltage and the current drawn were recorded using a 10 bit digitizer with a sampling

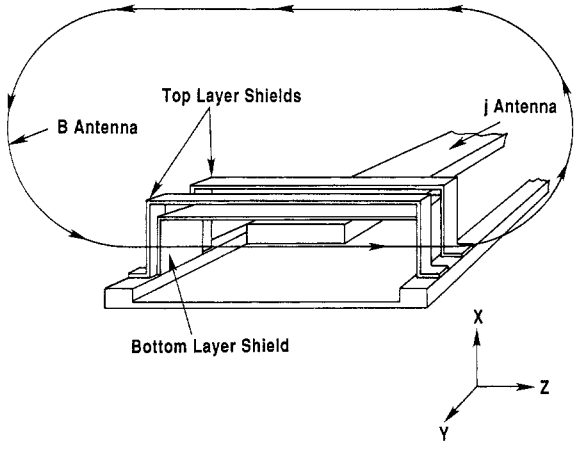

FIG. 1.—Faraday shield arrangement for the PLT ICRF antennas.

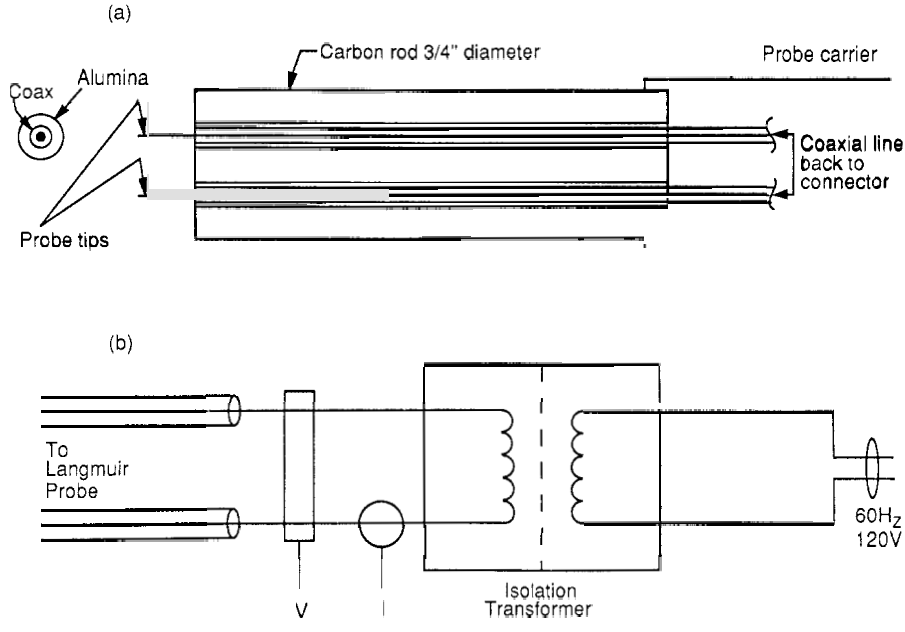

FIG. 2.—(a) Schematic diagram of the double Langmuir probe used for the edge density and temperature measurements. (b) Bias circuit for the double probe.

rate of 12.5 kHz. The electron temperature and density were obtained from the current–voltage (I–V) characteristic of the probe. When the collecting areas of each probe element are identical, the ideal probe characteristic (MANOS, 1985) is:

$$I = I_{\text{sat}} \tanh\left[\frac{eV}{2\text{k}\,T_e}\right].$$

The ion-saturation current, I_{sat}, was obtained from the probe current trace. T_e was then chosen to yield the best fit to the probe characteristic. The density was determined from:

$$n_e = \frac{2AI_{\text{sat}}}{C_s}$$

where A is the collecting area of the probe elements, and C_s is the ion sound speed, defined as:

$$C_s = \sqrt{\frac{2\text{k}\,(T_e + T_i)}{M_i}}.$$

For this analysis is was assumed that $T_e \approx T_i$ since the production of fast edge ions is not expected with ^{3}He minority heating (MANOS *et al.*, 1984). This allows the ion sound speed to be evaluated easily. The electron temperature was adjusted to give a

least-squares fit of the probe data to the ideal probe characteristic. As in other Tokamaks (LIEWER, 1985), the fluctuations in the edge parameters of PLT are a significant fraction of the mean values. In order to obtain the average plasma parameters, the data were digitally filtered using a finite impulse response (MCCLELLAN *et al.*, 1973) (FIR) filter. The bandwidth of the digital filter was adjusted so as to be able to resolve electron temperatures as low as 5 eV. If the bandwidth of the filter is too low, the slope of the *I–V* curve in the transition region will be decreased, masking the data as due to a higher electron temperature. Typical unfiltered *I–V* data and the least-squares fit to the ideal probe characteristic are shown in Fig. 3a. In Fig. 3b, the same data were digitally filtered. In both cases the least-squares fit was found at $T_e = 25$ eV. In most cases the data were filtered because the fluctuation level could be so large as to make a determination of the temperature impossible. The probe characteristic was found to be free of rectification for the available range of r.f. powers.

Optical spectroscopy has been widely used on Tokamak plasmas to characterize the edge region under a variety of plasma conditions (HINTZ and BOGEN, 1984; MCNEILL *et al.*, 1984). Spectroscopic measurements were used in this research to infer changes in the concentrations of deuterium and impurities in the edge region during ICRF heating. Light emitted during a discharge was collected by collimated fiber optics, filtered at specific wavelengths and then detected by photomultiplier tubes (PMT). The PMT outputs were used as measures of the intensities of the specific lines. The viewing spot of each of the collimated fibers was ~15 cm wide, slightly larger than the toroidal extent of the ICRF antennas. The Balmer-alpha line of

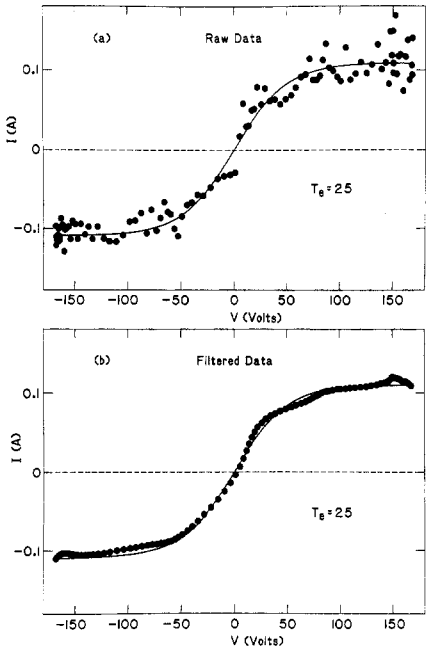

FIG. 3.—Double Langmuir probe data. (a) Raw data and the least-squares fit to the ideal probe characteristic. (b) Filtered data and the least-squares fit.

deuterium (656.2 nm) was used as a measure of neutral deuterium entering the discharge. The D_α line has been shown (MCNEILL, 1988/1989) to be a good measure of the neutral deuterium because the number of D_α photons emitted per entering deuterium atom is relatively constant over a wide range of plasma conditions. Although similar work has not been carried out for the visible lines of carbon, chromium and iron, these lines are often used to monitor the impurity production in plasma devices. Weber (1985) used visible lines of Cr I and C III on the ZT-40M device and found good agreement with the VUV spectrometry (which observes higher ionization states) for estimating the concentration of impurities. The visible lines are useful in localizing the source of impurities in Tokamak devices because the line emission is expected to be most intense near the source. Here the C III 464.7 nm, Cr I 425.4 nm, and Fe I 404.7 nm lines were used as indications of the amount of impurities entering the plasma. These lines result from neutral or partially ionized atoms colliding with low energy (< 100 eV) electrons. The line emission from these transitions is strongest in the edge region, close to the point of origin of the atoms. We assume that the number of visible photons per entering impurity ion remains relatively constant for the discharges studied here.

Optical fibers were positioned at various locations on PLT (Fig. 4). The fibers located at the TV Thomson Scattering (TVTS) port viewed perpendicular to the magnetic axis into an optical dump. Emission from this view represented the global behavior of various line spectra, and therefore was referred to as the "global" view. The fibers at gap 13 viewed toward the ICRF antennas located in gaps 17 and 18. Up to four fibers were used at gap 13 to view different poloidal locations on the antenna. The antenna in gap 17 could be viewed at four different locations from the bottom to the midplane. In addition, a fiber positioned at gap 18 had a grazing view of the side of the ICRF antenna.

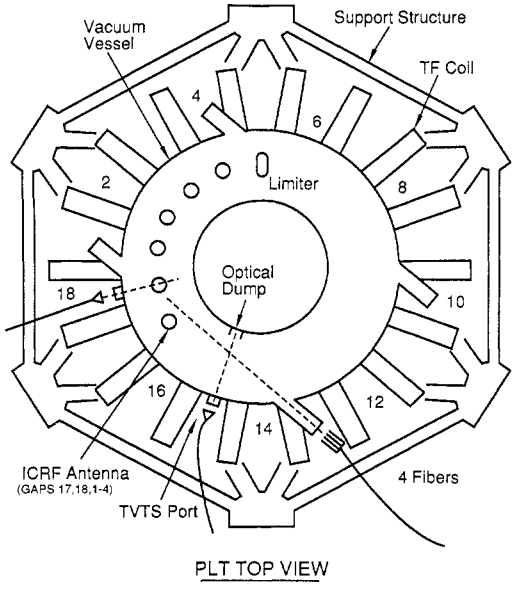

FIG. 4.—Location of the fiber optic viewing location on PLT.

3. EXPERIMENTAL MEASUREMENTS

3.1. *Main body plasma parameters*

The time evolution of I_p and $\bar{n}_e$ for a typical PLT discharge is shown in Fig. 5. After the discharge was initiated, additional deuterium was puffed into the vessel to maintain the desired plasma density. At 380 ms a small amount of ^{3}He was puffed into the discharge. The ICRF power was absorbed by the ^{3}He ions which in turn collisionally damped onto the bulk ion population (STIX, 1975). The minority ion concentration, estimated from the increase in $\bar{n}_e$, was between 5 and 10% of the total ion population. In this discharge, 800 kW of ICRF power was injected from 450 to 650 ms. The application of ICRF results in a density rise. This rise, which occurs with the gas feed closed, acts to fuel the discharge. The increase in density depends on the condition of the vacuum vessel and antenna structures. Immediately after a vacuum opening, the discharges are dirty (high Z_{eff}) and the density rise tends to be large. At times, the rise can be so large as to cause the plasma to disrupt. After some time, daily operation of the antennas and PLT results in a reduction of the density rise and allows the application of higher ICRF powers.

The application of ICRF power increases the deuterium temperature from 850 to 1400 eV, though negligible electron heating was observed. The ion temperature was measured with the CENA charge-exchange diagnostic (ROQUEMORE, 1985) and the electron temperature was measured with an electron cyclotron emission diagnostic. There was no indication of a fast population of ^{3}He ions being created, though at higher power levels or lower ^{3}He densities a fast population could be created which could then damp onto the electrons. Even then, the majority of the ICRF power is coupled to the bulk plasma ions. The ion temperature rose by approximately 70% and $\bar{n}_e$ increased by 30%; hence, the total ion stored energy increased by 120%. At the same time, the heating power (Ohmic + ICRF) increased by approximately 130%.

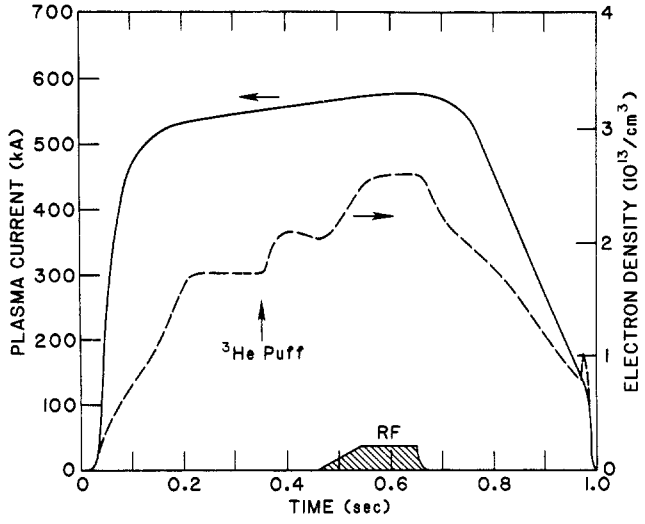

FIG. 5.—Plasma current and line-averaged density for a typical PLT discharge in which 800 kW of ICRF were applied.

Therefore, at these power levels, the ion energy confinement time exhibits negligible change.

For Tokamak ICRF heating experiments, the heating efficiency is defined by the heating quality factor $\Delta T_i \bar{n}_e / P_{r.f.}$. The discharge shown in Fig. 4 exhibits a heating quality factor of 1.8×10^{13} eV cm^{-3} kW^{-1}. This is about half the value quoted by MAZZUCATO *et al.* in 1984 for PLT discharges with $\bar{n}_e = 3.8 \times 10^{13}$ cm^3 and 2.6 MW of coupled ICRF power. The lower heating quality factor, and hence the lower energy confinement time of the present experiments, is believed to be due to greater radiative power loss. The proportional increase in radiative power was three times greater for this discharge than for the discharges described by Mazzucato. Impurity line radiation ruins the quality of the discharge by lowering the energy confinement time. Figure 6 shows the radiated power as measured by a bolometer viewing a central chord. The electron temperature exhibited little change during ICRF heating, thus the increase in radiated power was due to an increase in electron density and impurity density. Since the electron density increase was only 30%, the 125% increase in radiated power is attributed mainly to an increase in impurity concentration. Previous measurements of the radiation spectra in the range of 20–27 nm showed that the increased impurity concentration was mostly carbon, oxygen, iron, and titanium (WOUTERS *et al.*, 1965). There was a general increase in all of these lines so that the increased line radiation was caused by an increase in the density of impurities rather than a change in the ratio of emitting states. A bolometer was used as an indication of the purity of the discharges, since earlier work has shown that a bolometer provides a good measure of the impurity concentration (STRATTON *et al.*, 1984).

The condition of the vacuum vessel and antennas placed an operational limit on the maximum power-handling capability of the antennas. If either the machine was dirty or the antennas had not been energized recently, the application of ICRF resulted in an exceedingly large density rise accompanied by excessive impurity production. This in turn resulted in either the antennas arcing, or disruption of the discharge.

Figure 7 shows the variation in the line-averaged density rise for four separate days of operation. For each day a linear fit to the density rise data is shown for comparison. On 22 September 1986 the vessel had not been opened to atmosphere for approximately one month. ICRF heating experiments had been conducted for 3 days of the

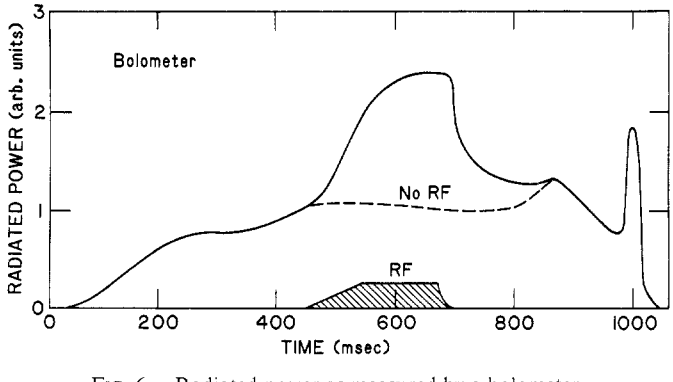

FIG. 6.—Radiated power as measured by a bolometer.

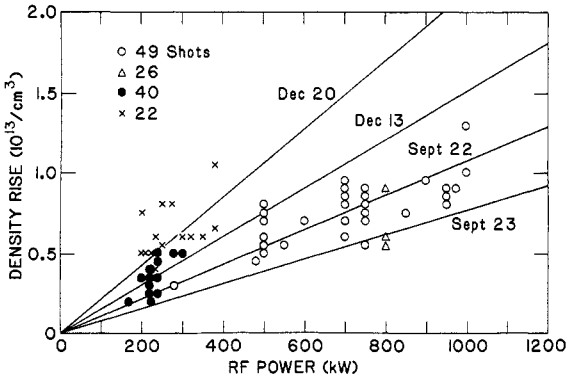

FIG. 7.—The density rise for four separate days of operations versus r.f. power. The scatter in the points for a given day results from changes in the vessel throughout the day. The number of shots plotted for each day is indicated.

prior week and the vacuum vessel and antennas were well conditioned. As the run day progressed, the size of the density rise decreased. On 23 September, the size of the density rise had further decreased and the discharges were very nearly reproducible. The vacuum vessel was in poor condition on 13 December as shown by the large scatter in the density rise data. The poor vessel condition was attributed to the vessel losing vacuum in mid-November. The density rise was exceedingly large on 20 December owing to a large number of impurity injection experiments conducted during the prior week. In contrast, the density rise for discharges reported by MAZZUCATO (1984) was approximately half as a large as on 23 September.

It is worth noting that even though the vacuum vessel and antennas were in good condition for the 1984 runs, the discharges suffered from the same problems as those of the lower power experiments of this research. Since the nature of the discharges was similar, these low-power experiments were appropriate for investigating the deleterious side-effects of ICRF heating.

3.2. *Edge plasma parameters*

3.2.1. *Edge density and temperature measurements.* Figure 8a shows the edge density profile for discharges in which 800 kW of ICRF was applied. These data were taken on 23 September on discharges in which $\bar{n}_e$ rose from 2×10^{13} to 2.6×10^{13} cm^{-3} with the application of ICRF. The double Langmuir probe was located in the horizontal midplane, approximately 80° toroidally away from one of the energized antennas. In this location, the probe could only extend to a minor radius of 42.3 cm. The location of the outer blades of the Faraday shield is also shown. The edge density fell rapidly at radii greater than the antenna radius because the average connection length, defined as the distance along a field line between limiting surfaces, was reduced by a factor of three. This reduction was due to the four antennas that were present in PLT on this run day.

The line-averaged density increased by 30%, while the edge density increase was much greater. For minor radii from $r = 42.3$ to 43.5 cm the density increased by 70%, and for $r > 43.5$ cm the density increase was even greater. Figure 8b shows the

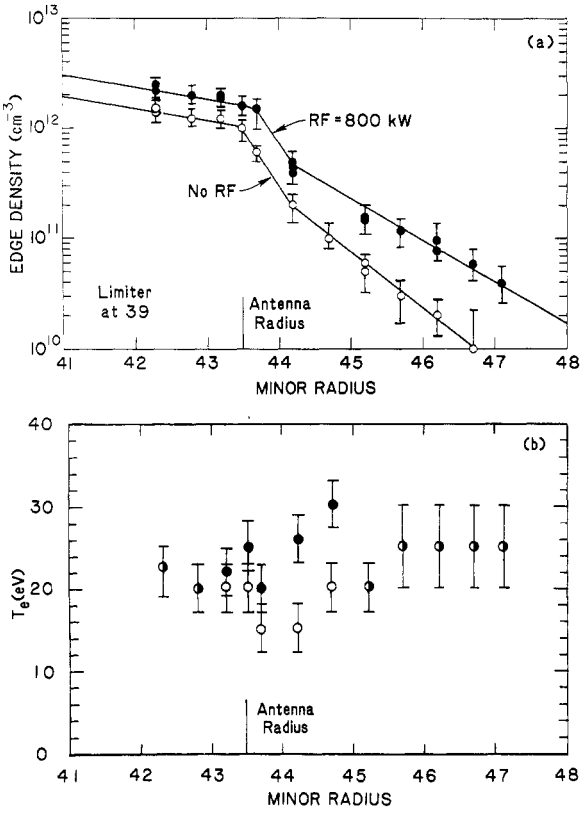

FIG. 8.—Radial profile of edge density and temperature before and during the application of ICRF. These data are from discharges taken on 23 September 1986.

average electron temperature including error bars representing the variation in the temperature. The temperature is nearly constant throughout the edge without ICRF. This is to be expected because the mean-free path of an electron in the edge is approximately 5 m, comparable to the distance between limiters. During ICRF heating, there was some indication of electron heating at the radial location of the Faraday shield blades. The increase in the electron stored energy in the edge was thus in excess of 30%. These data will be compared to data taken with the probe located at the bottom of the vessel, 180° away from the energized antenna.

To investigate the differences between gas-puff fueling and the ICRF-induced density rise, the density control system was programmed to mimic the density rise observed during ICRF heating. The edge density and temperature profiles for the gas-puff experiment are shown in Fig. 9. The edge density shows a slight increase, but the increase is much smaller than with ICRF. The temperature shows little change, except possibly at $r = 42.3$ cm. The change in the electron stored energy in the edge region was negligible, in contrast to the edge conditions in which 800 kW of ICRF was applied.

The Langmuir probe was moved from the midplane port near the antenna to a port

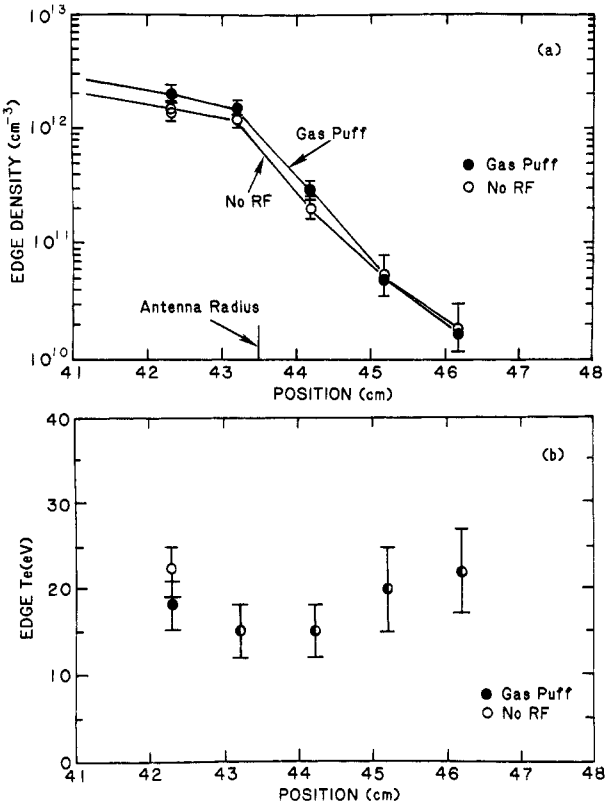

FIG. 9.—Edge density and temperature profiles for the gas-puff experiment.

at the bottom of the vessel in order to compare the edge parameters at both locations. The bottom port was approximately 180° away toroidally from the antennas. During this run period, the highest ICRF power achieved was only 300 kW, a limit set by arcing of the antennas. The Ohmic level of radiated power was twice that of the prior run period, suggesting that the machine was dirty. Figure 10 shows the edge density and temperature profiles for discharges with 300 kW of ICRF power applied. The line-averaged density for these discharges was initially 2.9×10^{13} cm^{-3}, and increased to 3.4×10^{13} cm^{-3} with the application of ICRF. While $\bar{n}_e$ rose by 17%, the edge density rose by over 30%. The decay of the density at the bottom of the machine was less severe than at the midplane. The midplane probe position intersected flux lines that terminated on the side of a nearby antenna, while at the bottom of the vessel, the flux lines wrapped around to the other side of the vessel before intersecting an antenna or other limiting surface.

The temperature at the bottom port exhibited little change with the application of ICRF. This is in contrast to the midplane port measurements which indicated a temperature increase at minor radii near the location of the Faraday shield blades. In order to determine if edge heating occurred near the Faraday shield surface, the change in electron temperature during ICRF heating was plotted versus radial

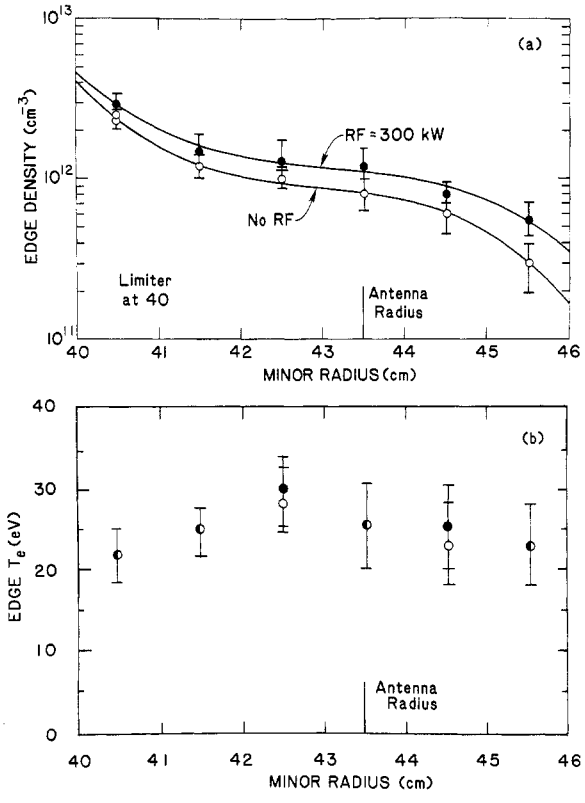

FIG. 10.—Radial profile of edge density and temperature before and during the application of ICRF. These data are from discharges taken on 13 December 1986.

position. Figure 11 shows the average change in electron temperature plotted with error bars equal to ± 1 standard deviation. O and I indicate the location of the outer and inner blades of the Faraday shield. The comparison is made between bottom and midplane probe positions, although the r.f. powers were not identical. The probe measurements in the bottom port (300 kW) show no clear change in the electron temperature; however, the measurements taken at the midplane port (800 kW) indicate that electrons were being heated near the shield surface. The temperature change appears to be greatest at $r = 44.5$ cm, 5 mm behind the inner blade of the Faraday shield, although the relative position of the antenna to the probe is only known within 5 mm. This is the only clear trend that has been observed in electron temperature. An explanation for electron heating in the vicinity of the Faraday shield has been proposed by LEHRMAN (1988). The finite parallel electric field that exists as a consequence of fast wave excitation is expected to heat electrons which transit close to the surface of the Faraday shield.

To further investigate changes in the edge, the limiter position was changed from 40 to 42 cm. This was the largest minor radius that could be achieved without risking damage to the antennas or other vacuum vessel components. The character of the discharge was not changed with the larger limiter radius. The line-averaged density

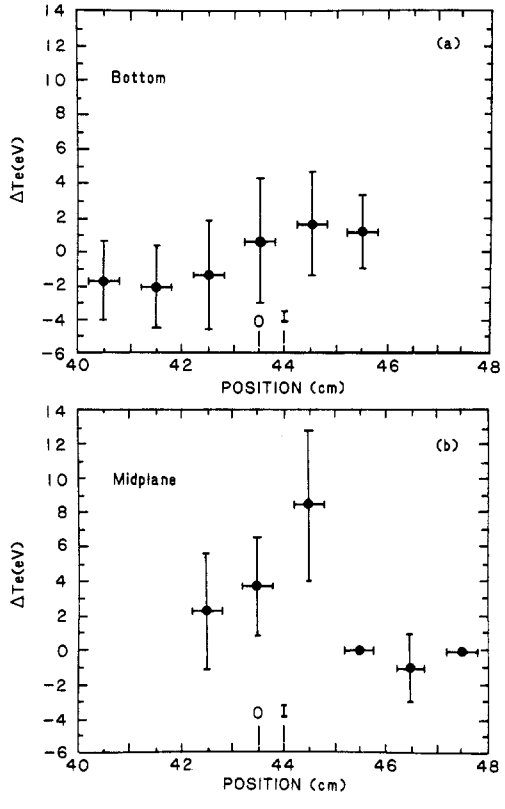

FIG. 11.—Average change in electron temperature with the application of ICRF. The vertical error bars are ±1 standard deviation and the horizontal error bars are equal to the radial extent of the Langmuir probe collecting element. O and I indicate the location of the inner and outer Faraday shield blades. (a) Probe located in the bottom port (300 kW). (b) Midplane port (800 kW).

rose from 2.4×10^{13} to 2.8×10^{13} cm^{-3} with the application of 250 kW of ICRF. The behavior of the edge density and temperature was similar to Fig. 10, although the probe measurements could only be made up to 42.5 cm to avoid destroying the Langmuir probe. No observable change was seen in the electron temperature, while the edge density increased by approximately 40%.

The toroidal magnetic field was varied from 23.5 to 32.5 kG to determine if magnetic field strength changed the character of the edge plasma. The change in toroidal field shifts the location of the ion-hybrid layer from a few centimeters within the magnetic axis to $r = 30$ cm on the inboard side of the vessel. For 300 kW ICRF discharges, the behavior of the bulk plasma was similar for this range of toroidal magnetic fields and there was no significant difference in the behavior of the edge plasma.

Plasma current was varied from 440 to 670 kA and again there was no observable difference in either the bulk plasma parameters or the edge parameters. Additionally, $\bar{n}_e$ was varied from 1.2×10^{13} to 4.5×10^{13} cm^{-3} and there was negligible change in the edge density and temperature profiles from those of Fig. 10. These results suggest that under a wide range of conditions, the character of the edge plasma is uncorrelated

to the behavior of the bulk plasma. A similar result was found for the FT Tokamak (PERICOLI-RIDOLFINI, 1985).

3.2.2. *Spectroscopic observations.* The general behavior observed during ICRF heating was an increase in the D_α emission viewed both globally and at the antenna. Additionally, there was a similar increase in Cr I, C III, Fe I, and all other line spectra that could be identified during the Ohmic phase of the discharge. The level of the increase depended strongly on the condition of the antennas and vacuum vessel. The global behavior of D_α, C III, and Cr I versus ICRF power, for discharges taken on 22 September (clean machine conditions), is shown in Fig. 12. Each of the lines has been normalized to its Ohmic value so that the rate of rise of each could be compared. The increase in D_α was correlated with the density rise, while the increase in C III and Cr I was correlated with an increase in impurity concentration and hence an increase in radiated power. Though not monitored on this day, the behavior of iron was typically similar to that of chromium. The scatter in the spectroscopic data was a result of the changes in vessel conditions during the day and was similar to the behavior in the density rise for that day (Fig. 7). An important result of this measurement was that the increase in the rate of production of chromium (iron) was greater than the for carbon and deuterium. The relative rates were 2.7 : 1.4 : 1.0 for chromium : carbon : deuterium.

The experiment was repeated the following day for 800 kW ICRF and gas-puff simulation discharges. For the 800 kW discharges, chromium increased by 240% with the relative rates of production of Cr : C : D being 2.5 : 1.2 : 1.0. For the gas-puff experiment, chromium increased by 60% with the relative rates of production for Cr : C being 1.4 : 1.2. The rise in D_α for the gas-puff experiments is not included because a gas inlet in a nearby port obscured these data. The difference in chromium production for the two experiments is of great concern. In the case of gas puffing, the chromium production was similar to the carbon production, while in the case of ICRF heating, the chromium production was more than twice as large as the carbon production. This preferential increase in metallic impurities could severely limit the usefulness of ICRF at higher power levels. The increased impurity production in the gas puff case is believed to be due to an increase in the particle flux to the limiters and

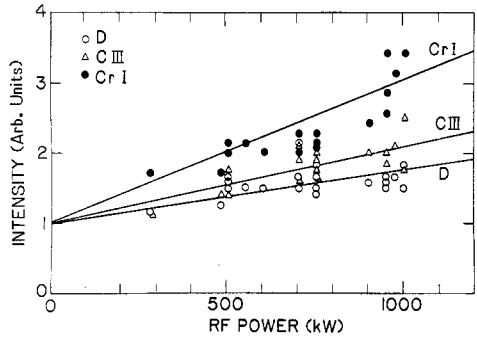

FIG. 12.—Intensity of D_α, C III, and Cr I versus r.f. power for discharges taken on 22 September 1986. Each line has been normalized to the Ohmic emission level for comparison of the relative rates of production.

vessel wall, since the auxiliary heating power was roughly constant. For the ICRF case, the heating power doubled which, in turn, should double the energy deposition. One explanation for the density rise and impurity generation might be that an increase in power to the limiters and the vessel wall causes an increase in sputtering and gas desorption.

To determine whether the source of deuterium and impurities was global or localized to the antenna, an array of fibers viewing the antenna was used to compare the line emission globally and in the vicinity of the antenna. ICRF heating experiments were conducted utilizing six antennas and the power division between antennas was varied while the total coupled power remained constant. The time evolution of the D_α emission at one of the antennas is shown in Fig. 13. Emission for the case when 80 kW of the total 260 kW was applied to the viewed antenna was compared to the case in which no power was applied to the viewed antenna. In these discharges, $\bar{n}_e$ rose from 2×10^{13} to 2.8×10^{13} cm^{-3}. The Ohmic case is also shown for comparison. These discharges exhibited decreasing D_α emission with time. Note, that with 30% of the applied power on the viewed antenna, the increase in D_α emission was twice that observed when all of the power was applied to other antennas. Therefore, the increase in D_α emission at the energized antenna (local view) was ~ 4.5 times greater than the increase over the rest of the vessel (global view). A comparison was made of the Cr I to D_α emission viewing an energized antenna. The increase in Cr I was found to be 2.7 times the increase of D_α, the same ratio as in the global view.

It has been suggested that either the large inductive voltage that develops at the ends of the antenna, or heating of edge ions in the resonance layer that intersects the antenna, causes ions to be accelerated into the shield surface (OHKAWA *et al.*, 1985). Bombardment of the shield surface could then result in increased sputtering and desorption and produce the density rise and impurity generation associated with ICRF heating. To determine if the emission observed at the antenna was localized to either the middle or the ends of the antenna, approximately 150 discharges where produced while deuterium and chromium emission was monitored at the four locations (end to midplane) on the antenna. There was no clear difference in the relative increase in emission at the four different locations on the antenna.

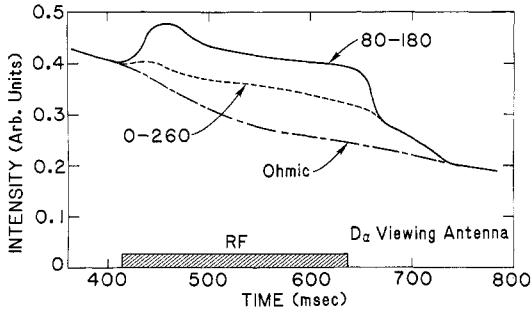

FIG. 13.—Time evolution of D_α viewing an ICRF antenna. The case of 80 kW applied to the antenna with 180 kW on other antennas is compared to the case of no power applied to the antenna with 260 kW applied to other antenna. Also shown is the case in which only Ohmic heating power is applied.

For discharges produced during a later run period when the machine was extremely dirty, the behavior of the line emission was similar to earlier observations, but the line emission from impurity atoms was approximately twice that when the machine was clean. A comparison was made for similar discharges in which the limiter position was changed from $r = 40$ to 42 cm. At 42 cm, the Faraday shield was only 1.5 cm behind the last closed flux surface. The D_α emission was greatest at the energized antenna with a similar increase in C III. The relative increase in the D_α emission near the energized antenna was ~ 3 times greater than the global increase. The emission levels show little change for the two limiter positions, in agreement with probe measurements which showed that the limiter position had little effect on the density or temperature in the edge region.

Antenna phasing experiments were performed on PLT to determine if the $n_\parallel$ spectrum had any pronounced effect on the generation of impurities. The r.f. systems could be operated to produce phase shifts between adjacent antennas of $\pm 60°$ and 180°. These phase shifts induced a parallel wave spectrum peaked at $n_\parallel$s of ± 2.7 and ± 8.2, respectively. The line-averaged density rise was similar for all the available phase shifts. The behavior of deuterium, viewing globally and at the antenna, and chromium, viewing the antenna, was unchanged for the available phase shifts. For these experiments, no clear change in the behavior of either the edge or bulk plasma was observed. These results are in contrast to those of JET in which a substantial increase in the metallic impurity production was observed when a large fraction of power was launched in waves with $k_\parallel = 0$–3 m^{-1} (BURES *et al.*, 1988). The difference between the two experiments could be attributed to the 0° phasing that was possible in the JET experiments, but was not possible in the PLT experiments. Experiments on TFTR (COLESTOCK *et al.*, 1989) and TEXTOR (BEUKEN *et al.*, 1988) have also exhibited more favorable heating when the antenna elements were run out-of-phase versus in-phase.

4. DEUTERIUM-EMISSION MODEL

In this section, the Langmuir-probe measurements of edge density and electron temperature are used in a model (MCNEILL *et al.*, 1987) which determines the D_α emission and electron-production profiles in the edge region for molecular deuterium released at the vacuum vessel wall and the Faraday shield. The model provides a correlation between the edge density and the D_α emission measurements and justifies the use of D_α as a measure of the particle source rate. The probabilities for ionization and dissociation are used to compute 1-D radial profiles of D_α emissivity and electron source rates. The local densities of D_2 molecules and D atoms, and the rates of production of D_α photons and electrons are computed. The model assumes a D_2 molecule is released from the vacuum vessel wall at a fixed velocity (e.g. corresponding to room temperature) and travels radially into the bulk plasma. The dissociation of D_2 results in slow and fast product atoms with energies of roughly 0.3 and 4 eV, respectively. The ratio of slow-to-fast dissociation products is assumed to be 1 : 2 (MCNEILL *et al.*, 1984). The resulting atoms travel with equal probability towards the wall or the interior. In this calculation dissociation product atoms are assumed to be reflected from the wall while charge exchange atoms stick there. Attenuation of charge exchange atoms in the plasma is through ionization alone. (This makes the source rates for D_α and electrons somewhat higher for charge exchange atoms). The

probability of ionization of the atomic products is then calculated. The production of first generation fast neutrals resulting from charge exchange with bulk plasma ions (assumed to have a fixed temperature) is also included. Along with the computed densities of D_2, D_2^+ and D atoms, the rate of production of D_α photons and electrons is computed.

Figure 14 shows the calculated profiles for D_α emission and electron production utilizing the temperature and density measurements from Ohmic discharges produced on 23 September (clean machine conditions). The limiter and Faraday shield radii are designated by L and A, respectively. According to the deuterium-emission model, 60% of the D_α emission from incoming molecules and product atoms is produced in the edge region (i.e. outside the limiter radius). The electron-production profiles indicate that 70% of the electrons are produced in the edge. This is consistent with

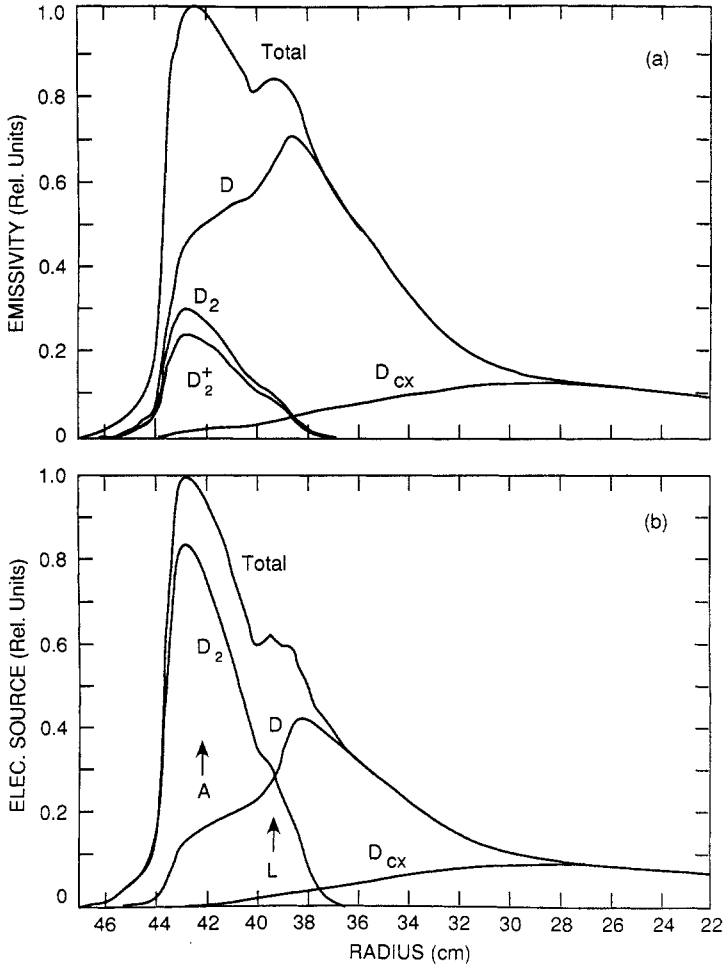

FIG. 14.—Calculated profiles for D_α emission and electron production for the Ohmic density and temperature profiles of Fig. 8. A and L are the locations of the antenna shield and limiter, respectively.

the edge density measurements which show that the particle fueling is much stronger in the edge region. The model was also used to calculate profiles for discharges in which 800 kW of ICRF power were applied. The electron and photon yields per molecule remained within 2% of the Ohmic values, but the maxima of the profiles shifted ~ 1 cm towards the wall. This shift results from the increase in edge density during ICRF heating, which reduces the mean-free path of the deuterium molecule and product atoms. The D_α emission and electron-production profiles at $r = 42$ cm are relatively flat, suggesting that, for a small shift in the profile the ratio of electron production to D_α emission should remain constant. Figure 15 shows that there is indeed a correlation between the edge density at $r = 42$ cm and the global D_α emission for both the Ohmic and ICRF portions of the discharge at moderate power levels. The fact that a correlation exists indicates that the global particle confinement did not change significantly (for these low-power experiments). The r.f. power was varied from 300 kW to 1 MW and $\bar{n}_e$ ranged from 1.9×10^{13} to 3.4×10^{13} cm^{-3} for these discharges.

The model was also used to determine the emission and electron-production profiles for molecules liberated from the surface of the Faraday shield. The profiles are similar to those of Fig. 14, with the maxima of similar shape, shifted out towards the limiter by 1 cm. The D_α emission from molecules released from the surface of the shield should be localized to a region within 4 cm of the shield. Therefore, the D_α emission from the antenna is roughly proportional to the rate of deuterons released from the surface of the Faraday shield.

5. CONCLUSIONS

Experimental measurements made during ICRF heating indicate that the edge density was significantly increased with the application of r.f. The temperature data indicate that local electron heating occurs in the vicinity of the Faraday shield of an energized antenna. The largest change in electron temperature occurred at the radial location of the inner shield blades. The edge electron stored energy increased in excess of 30% for 800 kW of coupled power, while gas-puff simulation discharges exhibit negligible change in the edge density and temperature, and thus the electron stored

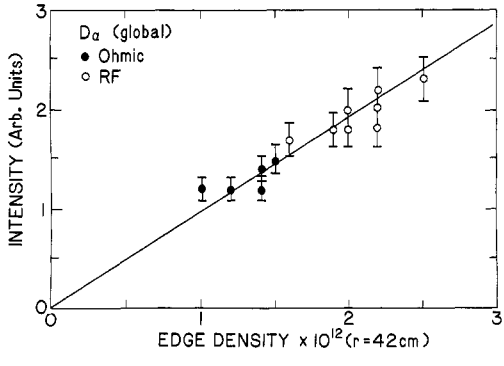

FIG. 15.—Edge density at 42 cm versus global D_α emission. ICRF powers ranged from 300 kW to 1 MW for these discharges.

energy. Spectroscopic measurements showed that the increase in metallic impurities during ICRF heating was larger than the corresponding increase in carbon or deuterium viewed both globally and at the antenna. The relative increase in the rates of production of Cr : C : D was 2.5 : 1.2 : 1.0 during ICRF heating. By contrast, the increase in the metallic impurities during the gas-puff simulation was similar to that of carbon, with relative production increases in Cr : C of 1.4 : 1.2, suggesting a difference in the mechanisms for impurity generation between ICRF and gas puffing.

According to one explanation for the density rise and impurity generation, an increase in power to the limiters and vessel wall was reponsible for an increase in sputtering and gas desorption. The problem with this explanation is that the measured emission from an energized antenna clearly demonstrates that the antenna is a significant source of impurities and deuterium. The correlation between the D_α emission and edge-density measurements suggest that D_α emission is localized and is a good measure of the particle source rate. The relative increase in emission at the energized antenna is ~ 3–4 times greater than globally. The generation of impurities and deuterium at the ends of the antenna was found to be no different than at the middle of the antenna. Thus, acceleration of edge ions due to resonant heating or an electrostatic field from the ends of the antenna are minor effects, if they occur at all. Spectroscopic measurements for antenna phasing experiments demonstrate that for the available phase shifts, the $n_\parallel$ spectrum had a minimal effect on the edge plasma. We conclude, therefore, that the transport in the vicinity of the energized antenna is significantly enhanced. The preferential increase in metallic impurities is explained by an increase in sputtering, resulting from elevated electron (and presumably ion) temperatures in the vicinity of the energized antenna.

Acknowledgements—This work was supported by Princeton University under U.S. Department of Energy contract No. DE-AC02-76-CHO3073 and the Grumman Corporation.

REFERENCES

ADAM J. (1987) *Plasma Phys. Contr. Fusion* **29**, 443.
BEUKEN J.-M., DE KEYSER L., DELVIGNE T. *et al.* (1988) *European Conf. on Controlled Fusion and Plasma Heating*, Dubrovnik, May 1988, 774.
BURES M., BRINKSCHULTE H., JACQUINOT J., LAWSON K. D., KAYE A. and TAGLE J. A. (1988) *Plasma Phys. Contr. Fusion* **30**, 149.
COLESTOCK P. L. (1984) *IEEE Trans. Plasma Sci.* **PS-12**, 64.
COLESTOCK P., CAVALLO A., DORLAND W. *et al.* (1989) ICRF and ICRF plus neutral beam heating experiments on TFTR, in *Applications of Radio-Frequency Power to Plasmas* (edited by R. MCWILLIAMS), Irvine, CA. AIP, New York.
COLESTOCK P. L., COHEN S. A., HOSEA J. C. *et al.* (1985) *J. Vac. Sci. Technol.* **A3**, 1211.
FURTH H. P. (1979) *Sci. Am.* **51**, 241.
GROVE D. *et al.* (1976) Experimental results of the PLT Tokamak, in *Conf. on Plasma Physics and Controlled Nuclear Fusion Research*, Berchtesgarden, IAEA-CN-35/A2, 21.
HINTZ E. and BOGEN P. (1984) *J. Nucl. Mater.* **128–129**, 229.
LEHRMAN I. S. (1988) A study of coupling and edge processes for ICRF antennas. Ph.D. dissertation, University of Wisconsin–Madison.
LIEWER P. C. (1985) *Nucl. Fusion* **25**, 543.
MANOS D. M. (1985) *J. Vac. Sci. Technol.* **A3**, 1059.
MANOS D. M., STANGEBY P. C., BUDNY R. V. *et al.* (1984) *J. Nucl. Mater.* **129**, 319.
MAZZUCATO E., BELL, R., BITTER M. *et al.* (1985) in *Proc. Tenth International Conf. on Plasma Physics and Controlled Nuclear Fusion Research*, London, paper F-I-2. IAEA Vienna (1985).
MCCLELLAN J. H., PARKS T. W. and RABINER L. R. (1973) *IEEE Trans. Audio Electroacoust.* **AU-21**, 97.
MCNEILL D. H. (1988) Princeton Plasma Physics Laboratory Report PPPL-2546 (August 1988); *J. Nucl. Mater.* (1989) **162–164**, 476.

MCNEILL D. H., BELL M. G., GREK B. and LEBLANC B. (1984) *J. Vac. Sci. Technol.* **A2**, 689.
MCNEILL D. H., LEHRMAN, I. S., GREENE G. J. *et al.* (1987) Visible spectroscopy on r.f. heated discharges in the Princeton Large Torus, in *Applications of Radio-Frequency Power to Plasmas* (edited by S. BERNABEI and R. W. MATLEY), Kissimme, FL. AIP, New York.
MESSIAN A. M., BHATNAGAR V. P., DELVIGNE T. *et al.* (1986) *Plasma Phys. Contr. Fusion* **28**, 71.
MURAKAMI M., CALLEN J. D. and BERRY L. A. (1976) *Nucl. Fusion* **16**, 347.
OHKAWA T. *et al.* (1985) *IEEE Trans. Plasma Sci.* **PS-13**, 563.
PERICOLI-RIDOLFINIE V. (1985) *Plasma Phys. Contr. Fusion* **4**, 493.
RAWLS J. M. (1982) Radio frequency heating and current drive, in *U.S. FED-INTOR Activity* (edited by W. M. STACEY). Georgia Institute of Technology Report USA FED-INTOR 82-1.
RINGER D., WINTER J., ESSER H. G. *et al.* (1988) *European Conf. on Controlled Fusion and Plasma Heating*, Dubrovnik, May 1988, Ap. X.
ROQUEMORE A. L., GAMMEL G., HAMMETT G. W., KAITA R. and MEDLEY S. S. (1985) *Rev. Scient. Instrum.* **56**, 1120.
STEINMETZ K., SOLDER F. X., ECKHART D. *et al.* (1986) in *Plasma Physics and Controlled Nuclear Fusion Research 1986* (*Proc. 11th Int. Conf.*, Kyoto, 1986) **1**, p. 461. IAEA Vienna (1979).
STIX T. H. (1975) *Nucl. Fusion* **15**, 737.
STRATTON B. C., MOOS H. W., HODGE W. L. *et al.* (1984) *Nucl. Fusion* **24**, 767.
THOMPSON H. R., JR. (1984) Second harmonic ion cyclotron resonance heating by the fast magnetosonic wave on the PLT Tokamak. Ph.D. Dissertation, Princeton University.
WEBER P. G. (1985) *Physics Fluids* **28**, 3136.
WOUTERS A. W., SCHWOB J.-L., SUCKEWER S. *et al.* (1985) *Bull. Am. Phys. Soc.* **30**, 1573.